A STUDY ON SENSOR MODELING AND TRIANGULATION FOR AN AIRBORNE THREE LINE SCANNER

WON JO JUNG, Doctorial Student
JAMES S. BETHEL, Associate Professor
School of Civil Engineering
Purdue University
550 Stadium Mall Drive, West Lafayette, IN 47907-2051
wjung@purdue.edu
bethel@ecn.purdue.edu

ABSTRACT

From the end of the twentieth century, commercial vendors have introduced airborne three line scanners, instead of more traditional single line scanners. While ADS40 (Leica Geosystems) and TLS (STARLABO) placed CCD arrays on the focal plane in a single optical system, 3-DAS-1 and 3-OC (Wehrli & Associates) use three optical systems but rigidly fixed to each other. For this reason, we need to develop a photogrammetric model for three different cameras but moving together along a single flight trajectory. In this paper, we present a sensor model for such a three line scanner and a piece-wise polynomial trajectory model. Preliminary triangulation results show that when geometric constraints on the trajectory model are loosely weighted, the misclosures in the image space are around 3 pixels while misclosures were increased up to 9 pixels if the geometric constraints are strictly enforced.

INTRODUCTION

The scanning method known by the name of pushbroom has been successfully implemented both in spaceborne and airborne applications. From the end of twenty century, commercial vendors have introduced airborne three line scanners, instead of more traditional single line scanners. For example, the ADS40 has been jointly developed by LH systems and German Aerospace Center, DLR in 1998 (Sandau et al., 2000). In 2000, STALABO Corporation designed a three line scanner named TLS jointly with the Institute of Industrial Science, University of Tokyo (Gruen and Zhang, 2003). In 2004, 3-DAS-1, a digital photogrammetric three line scanner, was jointly developed by Wehrli & Associates and Geosystem (Wehrli et al., 2004). In addition to 3-DAS-1, Wehrli & Associates and Geosystem also introduced 3-OC digital oblique camera in 2006. These cameras, digital three line scanners, provide a stereo capability within a single strip and increase redundancy in aerial triangulation. In addition to this, real-time direct geo-referencing is possible in theory with the aid of GPS and an inertial sensor.

To acquire 3D information from a three line scanner, a sensor model must be developed for the aerial triangulation. Unlike frame photography, where all pixels in the image are exposed simultaneously, each line of pushbroom image is collected at a different instant of time (Lee et al., 2000). Hofmann (1988) introduced the three line concept. Ebner (1996) describes the modeling of a spaceborne system called MOMS. Etheridge (1977) makes a useful inventory of mathematical techniques for modeling airborne pushbroom sensors.

While ADS40 and TLS placed CCD arrays on the focal plane in a single optical system, 3-DAS-1 and 3-OC uses three optical systems but rigidly fixed to each other. For this reason, we need to develop a photogrammetirc model for three different cameras but moving together along a single flight trajectory. This paper presents some preliminary triangulation results based on the piecewise polynomial trajectory model with geometric constraints.

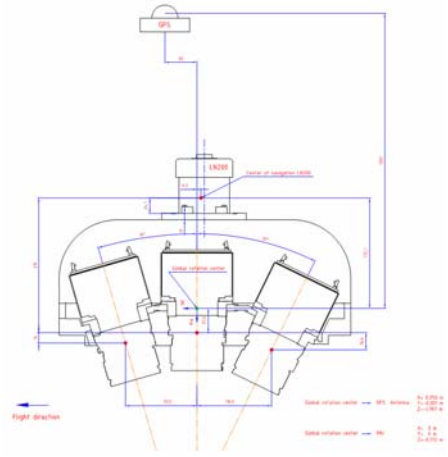

Figure 1. Sensor design.

3-DAS-1 Sensor Description

3-DAS-1 is an airborne three line scanner equipped with a GPS antenna and an inertial measurement unit (IMU). Three cameras are mounted on a stabilizer that is fixed at the bottom of the airplane. The IMU is firmly attached right above the camera system, and the lever-arm from the GPS antenna to the gimbal center is fixed in distance but not in attitude. Each camera has three linear arrays for color imaging, but this paper presents only geometric properties of 3-DAS-1 and radiometric characteristics are will not be considered. In this experiment, only the green band image of each camera is used for the triangulation. The nadir camera is looking down, the forward camera is tilted by 26 degrees and the backward camera is tilted by -16 degrees in the flight direction with respect to the nadir camera. The size of the CCD array is 8002 pixels, and the physical pixel size is $9\mu m \times 9\mu m$. Also, the focal lengths of all three cameras are identical, nominally $110mm$.

Coordinate systems

By the aid of the POS-AV system from Applanix Co. Ltd., the trajectory of the gimbal rotation center, SBET (Smoothed Best Estimated Trajectory), is acquired. SBET data provides locations in forms of latitude (λ), longitude (φ), and altitude (h) with respect to WGS-84 earth ellipsoid model. Locations are first transformed into the earth centered earth fixed (ECEF) coordinate system by equation 1 (Leick, 2004) and then transformed to the topocentric horizon coordinate system (THCS) at the origin of λ_0, φ_0 by equation 2 (Bugayevskiy and Snyder, 1995).

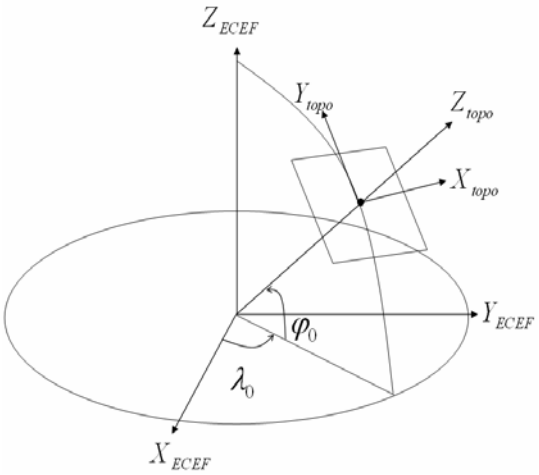

Figure 2. Earth coordinate system

$$
\begin{aligned}
X_{ECEF} &= (N+h)\cos\varphi\cos\lambda \\
Y_{ECEF} &= (N+h)\cos\varphi\sin\lambda \\
Z_{ECEF} &= \left(\frac{b^2}{a^2}N+h\right)\sin\varphi = ((1-e^2)N+h)\sin\varphi
\end{aligned}
\qquad \text{(Equation 1)}
$$

where, $a = 6378137.0$

1/f=298.257223563

b=a(1-f)

$$e=\sqrt{\frac{a^2-b^2}{a^2}}$$

$$N = \frac{a}{\sqrt{1-e^2\sin^2\varphi}}$$

$$
\begin{bmatrix} X_{topo} \\ Y_{topo} \\ Z_{topo} \end{bmatrix} = A' \begin{bmatrix} X_{ECEF} \\ Y_{ECEF} \\ Z_{ECEF} + e^2 N_0 \sin\phi_0 \end{bmatrix} - \begin{bmatrix} 0 \\ 0 \\ N_0 + H_0 \end{bmatrix}
\qquad \text{(Equation 2)}
$$

where

$$
A = \begin{bmatrix} -\sin\lambda_0 & -\cos\lambda_0\sin\phi_0 & \cos\lambda_0\cos\phi_0 \\ \cos\lambda_0 & -\sin\lambda_0\sin\phi_0 & \sin\lambda_0\cos\phi_0 \\ 0 & \cos\phi_0 & \sin\phi_0 \end{bmatrix}, H_0 = 0
$$

Attitude in SBET data is represented by three Euler angles, roll (ϕ), pitch(θ), and heading(ψ) with respect to the local body fixed coordinate system (X^b : along track, positive forward, Y^b : across track, positive to the right, Z^b :

vertical, positive to downward) and the navigation coordinate system (X^n : northward, Y^n : eastward, Z^n : vertical in the direction of the plumb line) as described in figure 3 (Baumker and Heimes, 2001). Since the test area is relatively small, the wander angle is neglected in this experiment so that angles are directly used in THCS. Since the 3-DAS-1 system records a time tag for each line of image, all the trajectory data in the form of X_{topo}, Y_{topo}, Z_{topo}, ϕ, θ, ψ is linearly interpolated with the time of imaging. Through this process, the location and attitude of the gimbal center at each image line is acquired.

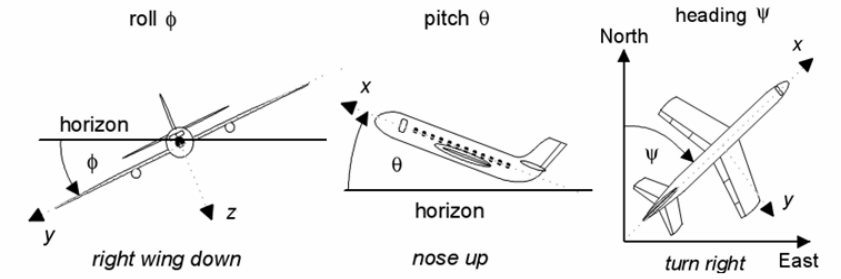

Figure 3. Attitude representation in three Euler angles (ϕ, θ, ψ) (Baumker and Heimes, 2001).

Sensor Model for a single line scanner

The objective of sensor modeling is to relate pixels in an image to coordinates in an orthogonal three-dimensional sensor coordinate system (SCS) (Lee et al., 2000). For line scanners, each line has its instantaneous perspective center. Then a pixel coordinate, line u and column v, can be transformed into the image coordinate system by equation 3. Then we can build a collinearity equation between an object coordinate in THCS and the corresponding image coordinate in SCS using equation 4.

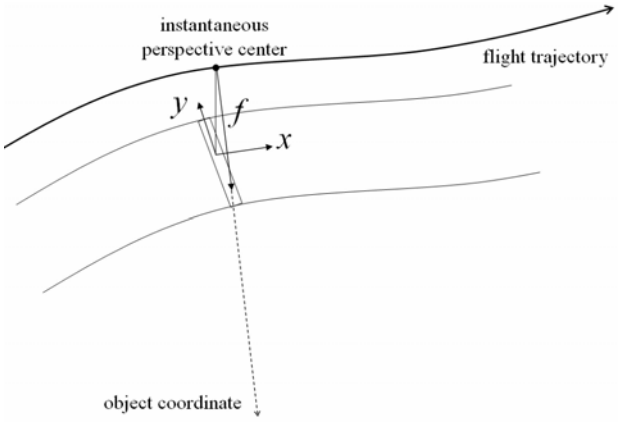

Figure 4. Imaging geometry.

$$x = (u - \text{int}(u)) \times 9\mu m$$
$$y = (v - 4000.5) \times 9\mu m \qquad \text{(Equation 3)}$$

$$\begin{bmatrix} x - x_p \\ y - y_p \\ -f \end{bmatrix} = \lambda M \begin{bmatrix} X - X_L \\ Y - Y_L \\ Z - Z_L \end{bmatrix} \qquad \text{(Equation 4)}$$

In equation 4, (X, Y, Z) is three dimensional ground coordinate in THCS and (X_L, Y_L, Z_L) is the location of an instantaneous perspective center in THCS. M is a 3 by 3 rotation matrix which relates an instantaneous SCS and THCS and λ is a scale factor. (x_p, y_p) is the principal point and f is the focal length of the camera. Then we could get two condition equations for an image point by equation 5.

$$F_x = x - x_p + f\frac{U}{W} \qquad F_y = y - y_p + f\frac{V}{W} \qquad \text{where, } \begin{bmatrix} U \\ V \\ W \end{bmatrix} = M \begin{bmatrix} X - X_L \\ Y - Y_L \\ Z - Z_L \end{bmatrix} \qquad \text{(Equation 5)}$$

Sensor Model for three line scanner

Based on the model for a single line scanner, we need to merge three camera models into a single, integrated model. Since the centers of projection of three cameras are fixed in the navigation coordinate system with respect to the origin of the instantaneous gimbal rotation center, we could estimate the location of the instantaneous perspective center of each camera using a 6 parameter transformation (three translations and three rotations). Since the forward and backward camera are tilted, we need to multiply by a rotation matrix to obtain forward and backward SCS as in equation 7. Then M matrix can be used for all three cameras. Finally, we could get 6 condition equations per one ground point in the form of equation 8.

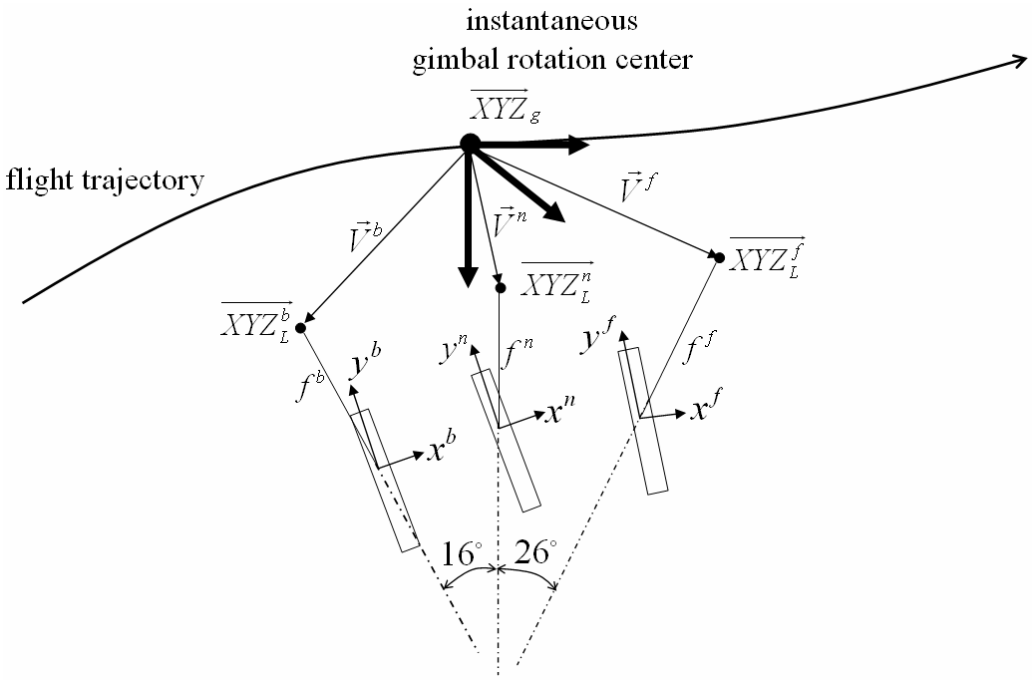

Figure 5. Imaging geometry of three line scanner.

$$\begin{aligned}\overrightarrow{XYZ_L^f} &= R(\phi,\theta,\psi)\vec{V}^f + \overrightarrow{XYZ_g} \\ \overrightarrow{XYZ_L^n} &= R(\phi,\theta,\psi)\vec{V}^n + \overrightarrow{XYZ_g} \\ \overrightarrow{XYZ_L^b} &= R(\phi,\theta,\psi)\vec{V}^b + \overrightarrow{XYZ_g}\end{aligned} \qquad \text{(Equation 6)}$$

where, $R(\phi,\theta,\psi)$ is 3×3 rotation matrix

$$R_y(26^\circ)\begin{bmatrix} x^f - x_p^f \\ y^f - y_p^f \\ -f^f \end{bmatrix} = \lambda M \begin{bmatrix} X - X_L^f \\ Y - Y_L^f \\ Z - Z_L^f \end{bmatrix}, \text{where} \begin{bmatrix} X_L^f \\ Y_L^f \\ Z_L^f \end{bmatrix} = \overrightarrow{XYZ_L^f}$$

$$\begin{bmatrix} x^n - x_p^n \\ y^n - y_p^n \\ -f^n \end{bmatrix} = \lambda M \begin{bmatrix} X - X_L^n \\ Y - Y_L^n \\ Z - Z_L^n \end{bmatrix} \qquad \begin{bmatrix} X_L^n \\ Y_L^n \\ Z_L^n \end{bmatrix} = \overrightarrow{XYZ_L^n} \qquad \text{(Equation 7)}$$

$$R_y(-16^\circ)\begin{bmatrix} x^b - x_p^b \\ y^b - y_p^b \\ -f^b \end{bmatrix} = \lambda M \begin{bmatrix} X - X_L^b \\ Y - Y_L^b \\ Z - Z_L^b \end{bmatrix} \qquad \begin{bmatrix} X_L^b \\ Y_L^b \\ Z_L^b \end{bmatrix} = \overrightarrow{XYZ_L^b}$$

$$F_x^f = x^f - x_p^f + f^f \frac{U^f}{W^f} \quad \text{where,} \quad \begin{bmatrix} U^f \\ V^f \\ W^f \end{bmatrix} = R_y^T(26^\circ) M \begin{bmatrix} X - X_L^f \\ Y - Y_L^f \\ Z - Z_L^f \end{bmatrix}$$

$$F_y^f = y^f - y_p^f + f^f \frac{V^f}{W^f}$$

$$F_x^n = x^n - x_p^n + f^n \frac{U^n}{W^n} \qquad \begin{bmatrix} U^n \\ V^n \\ W^n \end{bmatrix} = M \begin{bmatrix} X - X_L^n \\ Y - Y_L^n \\ Z - Z_L^n \end{bmatrix} \qquad \text{(Equation 8)}$$

$$F_y^n = y^n - y_p^n + f^n \frac{V^n}{W^n}$$

$$F_x^b = x^b - x_p^b + f^b \frac{U^b}{W^b} \qquad \begin{bmatrix} U^b \\ V^b \\ W^b \end{bmatrix} = R_y^T(-16^\circ) M \begin{bmatrix} X - X_L^b \\ Y - Y_L^b \\ Z - Z_L^b \end{bmatrix}$$

$$F_y^b = y^b - y_p^b + f^b \frac{V^b}{W^b}$$

where, $R_y(\alpha)$ is a α degree rotation with respect to the y-axis of SCS

Trajectory Modeling

Since the location of the perspective center and the attitude of each camera are determined by the location and the attitude of the gimbal, we model the trajectory of the gimbal rotation center instead of modeling three independent perspective centers. Because the time interval between exposures of adjacent lines of image is almost constant, the trajectory can be represented by a function of line number instead of actual exposure time. To avoid numerical instability, line numbers are normalized. At each polynomial section boundary, the zero order and the first order continuity constraints are enforced so that a smooth trajectory is guaranteed. The zero order constraint enforces the computed trajectory value at the boundary between two adjacent polynomial sections to be the same. And the first order constraint enforces the slope be the same at the borders. Figure 6 is the example of trajectory model for X_g.

$$
\begin{aligned}
X_g &= X_g^{\text{interpolated}} + dX_g(l) \\
Y_g &= Y_g^{\text{interpolated}} + dY_g(l) \\
Z_g &= Z_g^{\text{interpolated}} + dZ_g(l) \\
\phi &= \phi^{\text{interpolated}} + d\phi_g(l) \\
\theta &= \theta^{\text{interpolated}} + d\theta_g(l) \\
\psi &= \psi^{\text{interpolated}} + d\psi_g(l)
\end{aligned}
\quad \text{where,} \quad
\begin{aligned}
dX_g(l) &= X_0^i + X_1^i \cdot l + X_2^i \cdot l^2 \\
dY_g(l) &= Y_0^i + Y_1^i \cdot l + Y_2^i \cdot l^2 \\
dZ_g(l) &= Z_0^i + Z_1^i \cdot l + Z_2^i \cdot l^2 \\
d\phi(l) &= \phi_0^i + \phi_1^i \cdot l + \phi_2^i \cdot l^2 \\
d\theta(l) &= \theta_0^i + \theta_1^i \cdot l + \theta_2^i \cdot l^2 \\
d\psi(l) &= \psi_0^i + \psi_1^i \cdot l + \psi_2^i \cdot l^2
\end{aligned}
$$

$$l = \frac{(u - \text{image height}/2)}{\text{image height}}$$

$$\begin{bmatrix} X_g & Y_g & Z_g \end{bmatrix}^T = \overrightarrow{XYZ_g}$$

i : polynomial section number

(Equation 9)

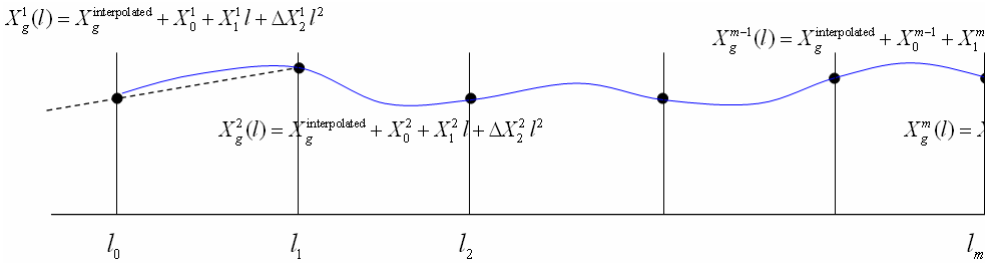

Figure 6. Example trajectory model for X_g .

Test data set and aerial triangulation result

Among twelve flights in the area of eastern Switzerland, we have decided to test one flight covering the St. Gallen area before getting involved with the entire data set. Unfortunately, we were unable to obtain any ground control and check point data. For the aerial triangulation, a total of 82 pass points were manually measured. After getting the initial approximations of ground coordinates using space intersection, we fixed 5 components of the ground points to avoid datum deficiency in the data adjustment. In this experiment, a total of 15 polynomial sections are used. After the least squares adjustment with continuity constraints using equation 10, we obtain the result shown in Table 1. In equation 10, the unknowns are the polynomial coefficients and ground point coordinates of the pass-points. For the self calibration, several internal parameters are also considered as free parameters. B is a Jacobian matrix of condition equations with respect to unknowns and C is a Jacobian matrix of constraint equations with respect to related polynomial coefficients.

$$
\begin{aligned}
v + B\Delta &= f \\
C\Delta &= g
\end{aligned}
\qquad \text{(Equation 10)}
$$

Table 1. misclosures in the images.

	RMSE in pixel		
	forward	nadir	backward

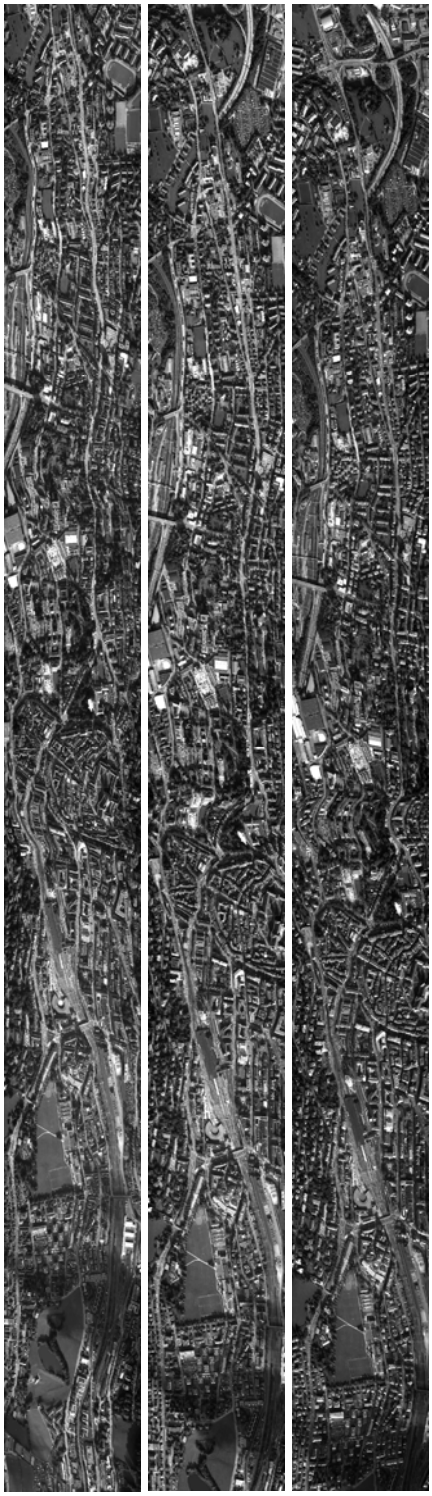

(a) forward (b) nadir (c) backward
Figure 7. Images (88068×8002 **pixels)**

	x	y	x	y	x	Y
weighted constrained	1.387	2.655	3.008	1.707	2.614	1.844
strictly constrained	4.027	3.243	8.903	1.662	6.012	2.395

Conclusion and Future works

In this experiment, we tested the model for a three line scanner using single flight of data. Even though the aerial triangulation is done without ground control information, the results show anticipated misclosures consistent with the piecewise polynomial method. This means the proposed model is able to recover a refined sensor trajectory. Since the polynomial trajectory model is very weak for abrupt changes, we would like to apply a stochastic model for the trajectory. We expect a stochastic trajectory model can reduce misclosures because it is more accommodating than a polynomial model for a rapidly varying trajectory. We are also planning to add additional internal camera parameters to the sensor model and , via self calibration, estimate refined trajectories and camera geometry for the remaining eleven flights.

REFERENCES

Baumker M, and F. J. Heimes, (2001). New Calibration and Computing Method for Direct Georeferencing of Image and Scanner Data Using the Position and Angular Data of an Hybrid Inertial Navigation System. OEEPE Workshop, Integrated Sensor Orientation, Hannover 2001.

Bugayevsiy, L. M. And J. P. Snyder, (1995). Map Projections : A Reference Mannual, Taylor & Francis Inc., Philadelphia., p.3.

Ebner, H., Ohlhof, T., Putz, E., (1996), Orientation of MOMS-02/D2 and MOMS-2P Imagery, *ISPRS International Archives of Photogrammetry and Remote Sensing, Commission III: 158-164*

Etheridge, M., (1977), *Analysis of Single and Double Coverage Aircraft Multispectral Scanner Arrays for Position Data*, PhD Thesis, Purdue University, May 1977

Gruen A., Zhang L., (2003). Sensor Modelling for Aerial Triangulation with Three-Line-Scanner (TLS) Imagery. *Journal of Photogrammetrie, Fernerkundung, Geoinformation, 2003* (2): 85-98.

Hofmann, O., (1988) A Digital Three Line Stereo Scanner System, *ISPRS International Archives of Photogrammetry and Remote Sensing, Kyoto, Commission II: 206-213*

Lee, C., H. J. Theiss, J. S. Bethel, and E. M. Mikhail, (2000). Rigorous Mathematical Modeling of Airborne Pushbroom Imaging Systems. *Journal of Photogrammetry and Remote Sensing, 66* (4): 385-392.

Leick, A., (2004). GPS Satellite Surveying, John Wiley & Sons Inc., Hoboken, New Jersey, pp. 367-378.

Sandau R., B. Braunecker, H. Driescher, A. Eckardt, S. Hilbert, J. Hutton, W. Kirchhofer, E. Lithopoulos, R. Reulke, and S. Wicki, (2000). Design Principal of the LH systems ADS40 Airborne Digital Sensor, Proceedings of IAPRS, Vol. XXXIII, Amsterdam, 2000, pp.258-265.

Wehrli H., V. Gayda, G. Wehrli, and J. Bethel, , (2004). Introduction of the 3-DAS-1 Digital Aerial Scanner, XXth ISPRS Congress, Commission 1, 12-23 July 2004, Istanbul, Turkey. http://www.isprs.org/istanbul2004/comm1/papers/100.pdf